

# Micro/nano spacecraft thermal control using a MEMS-based pumped liquid cooling system

Gajanana C. Birur<sup>a</sup>, Tricia Waniewski Sur<sup>b</sup>, Anthony D. Paris<sup>a</sup>,  
Partha Shakkottai<sup>a</sup>, Amanda A. Green<sup>a</sup>, and Siina I. Haapanen<sup>a</sup>

<sup>a</sup>Jet Propulsion Laboratory, California Institute of Technology, Pasadena, CA, USA

<sup>b</sup>Science Applications International Corporation, San Diego, CA, USA

## ABSTRACT

The thermal control of future micro/nano spacecraft will be challenging due to power densities which are expected to exceed 25 W/cm<sup>2</sup>. Advanced thermal control concepts and technologies are essential to keep their payload within allowable temperature limits and also to provide accurate temperature control required by the science instruments and engineering equipment on board. To this end, a MEMS-based pumped liquid cooling system is being investigated at the Jet Propulsion Laboratory (JPL). The mechanically pumped cooling system consists of a working fluid circulated through microchannels by a micropump. Microchannel heat exchangers have been designed and fabricated in silicon at JPL and currently are being tested for hydraulic and thermal performance in simulated microspacecraft heat loads using de ionized water as the working fluid. The microchannels are 50 microns deep with widths ranging from 50 to 100 microns. The hydraulic and thermal test data was used for numerical model validation. Optimization studies are being conducted using these numerical models on various microchannel configurations, working fluids, and micropump technologies. This paper presents background on the need for pumped liquid cooling systems for future micro/nano spacecraft and results from this ongoing numerical and experimental investigation.

**Keywords:** microchannel, microspacecraft, thermal control, electronics cooling, heat exchanger

## 1. INTRODUCTION

Future spacecraft used for deep space science exploration are expected to reduce in size by orders of magnitude. The size of the spacecraft currently used in deep space missions range from 500 to 2000 kg. National Aeronautics and Space Administration (NASA) is investigating reducing the size of the spacecraft to the order of 50 kg in the next five to ten years with a longer term goal of  $O(5\text{ kg})$ . Spacecraft of these sizes are referred to as micro/nano spacecraft; they are expected to have power levels from 10 to 50 Watts. Some of the space missions envisioned for these microspacecraft include missions to planets and moons such as Mars and Europa, missions to comets/asteroids, and Earth orbiting missions. These missions will utilize orbiter, flyby, rover, lander, and sample return vehicles. Also, NASA is sponsoring a program called the System-On-A-Chip program whose objective is to integrate the whole spacecraft on a single chip. A key challenge in designing and reliably operating future microspacecraft is providing effective thermal control to the high power density components on board so that their temperatures remain within allowable operating limits.

The power densities of the electronics, science instruments, and avionics in future microspacecraft are expected to exceed 25 W/cm<sup>2</sup>. This is an order of magnitude greater than traditional spacecraft designed and operated today; therefore, advanced thermal control technologies are required to meet the thermal requirements of the high power density components. Some of the technologies under consideration are high thermal conductivity materials, passive two-phase devices such micro heat pipes embedded in electronic packages, and thermo-electric coolers for active cooling. All of these technologies have limitations on how effectively they keep high power density electronic components below their upper temperature limit or how easily they integrate with heat dissipating components. A more promising thermal control technology is the MEMS-based pumped liquid cooling system, the focus of this paper. The MEMS-based pumped liquid cooling system consists of a working fluid circulated through microchannel heat exchangers by a micropump to remove heat (Fig. 1) from high power density electronic components. Then,

---

Further author information: (Send correspondence to G.C.B.)

G.C.B.: phone: 1 818 354-4762, fax: 1 818 393-1633, e-mail: Gajanana.C.Birur@jpl.nasa.gov

T.W.S.: phone: 1 858 826-2371, fax: 1 858 826-6592, e-mail: TRICIA.W.SUR@saic.com

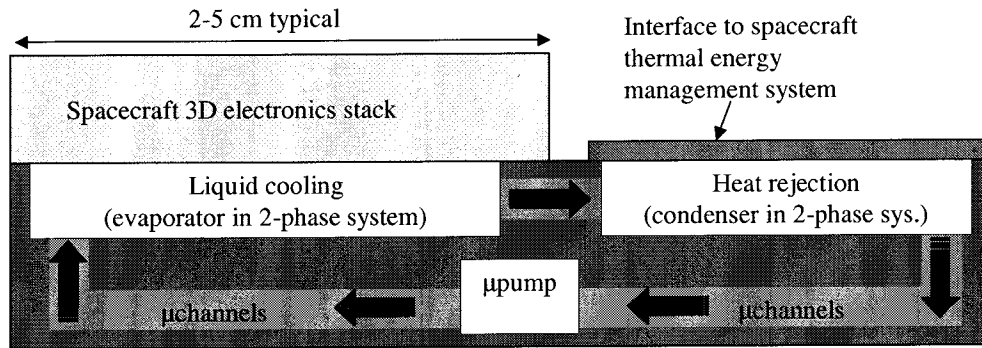


**Figure 1.** Schematic of the MEMS-based pumped liquid cooling system integrated with a 3D electronics stack.

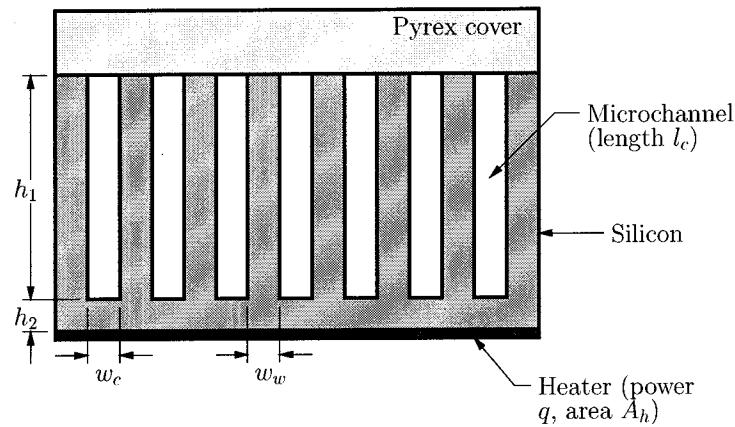


**Figure 2.** Microchannel heat exchanger schematic.

this heat can be transferred to a heat sink conveniently located away from the electronics where the spacecraft thermal control system can reject it at an external radiator. Some advantages of the MEMS-based pumped cooling system are: 1) increased effectiveness by integration of cooling system with payload, 2) increased freedom in locating electronics or science payload, 3) removal of large heat fluxes over large distances, 4) precision temperature control of electronics/payload by micropump flow control, and 5) ability to function in adverse gravity.

Using microchannel heat exchangers to remove heat from high power density electronics, lasers, and other equipment has been an active area of research since the seminal work of Tuckerman and Pease.<sup>8</sup> Their microchannel heat exchangers could remove  $1000 \text{ W/cm}^2$ ; however, the volumetric flow rate,  $Q$ , and the pressure drop,  $\Delta P$ , were both quite large. A review of more recent work was given by Goodling.<sup>9</sup> Figure 2 and Table 1 summarize some of these investigations where high heat fluxes were removed at the expense of large flow rates and pressure drops. There have been numerous investigations of two-phase liquid cooling systems as well. In general, two-phase systems require lesser flow rates but greater pressure heads to move vapor bubbles through the microchannels. Also, there is an additional risk associated with these systems that an uncondensed vapor bubble could enter the micropump and cause vapor lock. None of these systems are well-suited for microspacecraft thermal control where mass, volume, and power constraints restrict the choice of a pump to those which can provide much smaller flow rates and pressure heads.

This paper presents ongoing work from the development of a MEMS-based pumped liquid cooling system suitable for microspacecraft thermal control applications. The following sections discuss the topics of microspacecraft thermal control, design and fabrication of microchannel heat exchangers, numerical model development for microchannel heat exchangers and results, and experimental work.

**Table 1.** Comparison of rectangular microchannel heat exchangers for single-phase liquid water flow.<sup>1</sup> Entries in italics are calculated or estimated.

Investigators	Substrate	$A_h(A_c)$ cm <sup>2</sup>	$l_c$ cm	$h_1$ μm	$w_c(w_w)$ μm	$q$ W	$Q$ cc/s	$R_{total}$ °C/W	$\Delta P$ kPa
Harms <i>et al.</i> <sup>1</sup>	Silicon	6.25 (6.25)	2.5	1030	251 (119)	415	46.3	0.041	30.5
Tuckerman <sup>2</sup>	Silicon	1.0 (2.8)	1.40	302	50 (50)	790	8.6	0.090	214
Mahalingam <sup>3</sup>	Silicon	14.44 (25)	5.0	1700	200 (100)	<i>1050</i>	63	<i>0.018</i>	-
Kishimoto and Ohsaki <sup>4</sup>	Alumina	<i>16.0</i> (62)	8.6	400	800 (1740)	380	13.3	<i>0.132</i>	-
Sasaki and Kishimoto <sup>5</sup>	Silicon	<i>2.56</i> (4.8)	2.4	900	340 (340)	<i>416</i>	-	<i>0.120</i>	20
Riddle <i>et al.</i> <sup>6</sup>	Silicon	1.0 (3.0)	1.5	320	51 (53)	<i>2500</i>	18.0	<i>0.082</i>	500
Cuta <i>et al.</i> <sup>7</sup>	Copper	<i>4.06</i> (4.06)	2.05	1000	270 (270)	402.5	3.49	<i>0.168</i>	20.7

## 2. MICROSPACECRAFT THERMAL CONTROL

Microspacecraft thermal control design differs significantly from traditional, larger spacecraft thermal control design due to several reasons. First, since the spacecraft is much smaller in size, a single spacecraft component often is used for different functions. An example of this multi-functional approach is an avionics package that combines structural, electronic packaging, and thermal control functions. Second, heat fluxes from electronics and science equipment are an order of magnitude greater. Third, the heat capacity of a microspacecraft is small compared to the heat dissipated by the equipment. Furthermore, the power dissipating mode may last only a small fraction of the mission time. Thus, the thermal control system not only needs to remove high heat fluxes for short durations, but it also needs to conserve heat.

Solutions to the microspacecraft thermal control problem require different thermal control architectures than those of traditional spacecraft. Some of the thermal technologies needed are: 1) high heat flux removal from equipment, 2) high performance, light weight, thermal insulation, 3) deployable smart radiators, and 4) cooling loops that thermally couple all the spacecraft components. An advanced thermal control architecture that is being investigated at JPL<sup>10</sup> for both traditional and microspacecraft is shown in Figure 3. For microspacecraft, high heat flux removal technology is the most important, and pumped single-phase liquid cooling systems are very effective for this. Two liquid cooling system approaches may be used. The first approach uses an independent, MEMS-based pumped liquid cooling loop integrated with its own pump just for the electronics. Then, this loop is thermally coupled to the overall spacecraft thermal control system. The second approach uses the overall spacecraft pumped cooling loop and circulates the same fluid through high heat flux components to remove heat. The main advantage of the first approach is that it can be used on a microspacecraft irrespective of whether a cooling loop is used at the overall spacecraft level. Also, the MEMS-based pumped liquid cooling system can be directly integrated with the electronics, and (depending on the requirements) several of these can be used on a single microspacecraft. Furthermore, it eliminates the need for interconnects if an overall spacecraft cooling loop is used.

## 3. DESIGN AND FABRICATION

A key component of the MEMS-based pumped liquid cooling system is the parallel flow microchannel heat exchanger. The initial microchannel heat exchanger designs were based on those by the Stanford University Microfluidics Laboratory.<sup>11</sup> The footprint for these devices was approximately 3.5 cm<sup>2</sup>, typical of microspacecraft electronic components. Also, these devices feature integrated heaters so that heat loads typical of microspacecraft electronic components could be applied. A micropump will be used to circulate the working fluid through the microchannel heat exchangers; several technologies are under consideration.

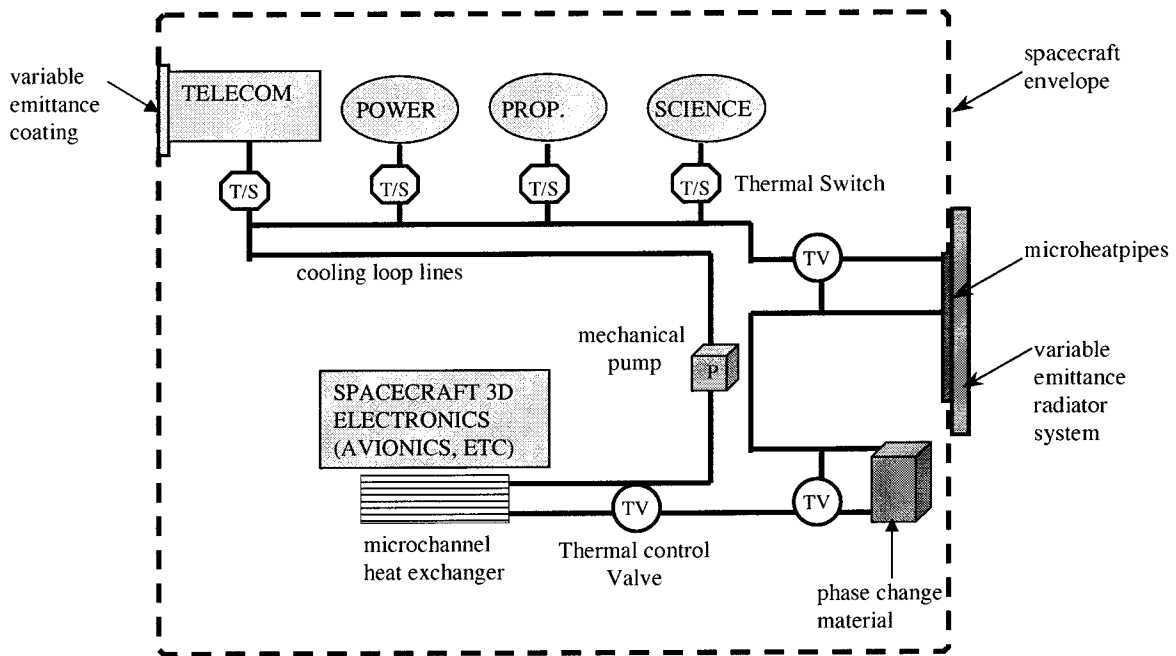


Figure 3. Advanced thermal control architecture schematic.

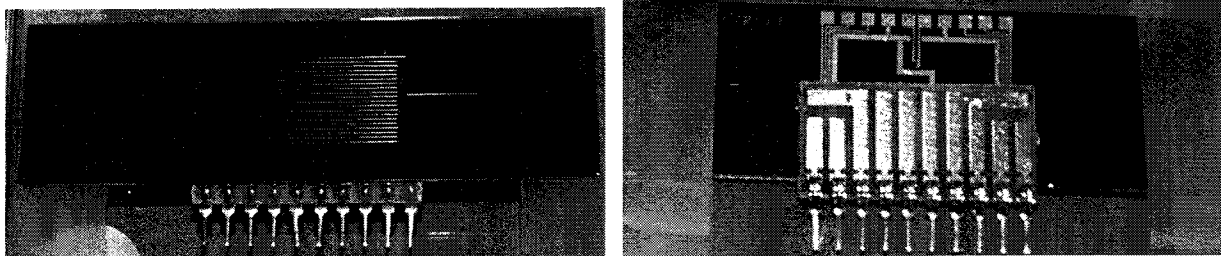


Figure 4. Microchannel heat exchanger device: front side (left) and back side (right). The front side shows the twenty microchannels and the manifolds etched in silicon. A piece of Pyrex 7740 glass bonded to the top seals the channels. The inlet and outlet holes are visible on the back side. Also visible are the aluminum tracks and pads for the electrical connections to the implanted heater strips (20) and thermistors (4). A surfboard with ten standard single inline pins is bonded to the back side and can be inserted into a Zero Insertion Force (ZIF) socket.

**Table 2.** Microchannel heat exchanger device parameters.

Device ID	100-50-30	75-50-50	50-50-20
number of channels	30	50	20
width, $w_c$ ( $\mu\text{m}$ )	100	75	50
spacing, $w_w$ ( $\mu\text{m}$ )	500	300	500
depth, $h_1$ ( $\mu\text{m}$ )	50	50	50
hydraulic diameter ( $\mu\text{m}$ )	67	60	50
length, $l_c$ (mm)	20	20	20
cooling area, $A_h$ ( $\text{cm}^2$ )	3.5	3.7	2.1

### 3.1. Design

Figure 4 shows the front and the back side of a typical microchannel device. For all the devices, the inlet and the outlet holes were 4 cm apart so that they could be easily interchanged in the experimental test fixture. The inlet and outlet manifold channels are 50 microns deep, 3 mm wide (to reduce pressure drop), and 1 cm long. For the device shown, there are 20 parallel rectangular cross-section microchannels in between the manifold channels. The microchannels are 50 microns wide, 50 microns deep, 2 cm long, and they are spaced 500 microns apart. Other devices had different microchannel widths and spacings. Three designs were fabricated and their dimensions are summarized in Table 2.

### 3.2. Fabrication

The microchannel devices were fabricated in the Microdevices Lab (MDL) at JPL using a similar process to the Stanford University Microfluidics Laboratory.<sup>11</sup> The devices were fabricated in four inch, double side polished silicon wafers that are 550 microns thick. The process begins on the backside of the wafer by patterning the resistors needed for the ion implantation. The ion implantation provides the high resistances needed for the thermistors and the heater. Core Systems, Inc. implanted  $1e15$  Boron+ at 40 Kev at a  $7^\circ$  tilt. Upon arrival back at MDL, a wet oxidation ( $950^\circ\text{C}$  for one hour) was used to drive in the implantation and grows approximately 2600 angstroms of oxide on the silicon. Contact windows were then patterned in the oxide and etched away using a 10:1 buffered oxide etch (BOE). Ohmic contact to the implanted resistors was provided by the deposition of aluminum traces 2550 angstroms thick. The wafer was then placed in a rapid thermal annealing system (RTP) for one hour with 10 slpm of  $\text{N}_2$  and 1 slpm of  $\text{H}_2$ . The manifolds and channels were then patterned on the front side of the wafer. A deep reactive ion etching system (DRIE) was used to etch the channels and manifold to a depth of 50 microns. Following the etching of the channels, the inlet/outlets are patterned and etched through on the backside of the wafer. Full wafer anodic bonding of a 500 micron thick Pyrex 7740 cover plate is used to seal the flow channels and allow for visual characterization. Dicing of the wafer releases the individual devices (three per wafer). Finally, electrical connections to the heater and thermistors is accomplished through the use of 25 micron diameter wire bonds to a ten pin single-in-line surfboard.

## 4. NUMERICAL MODEL

A numerical model was developed to predict the hydraulic and thermal performance of various microchannel heat exchanger devices. The model was based on MICROHEX, a FORTRAN code developed by Phillips.<sup>12</sup> For these devices, the microchannel hydraulic diameter is much greater than the molecular mean free path; therefore, the fluid behaves as a continuum. The major assumptions in the model are: steady and incompressible coolant flow, spatially and temporally constant power dissipation, isotropic thermal conductivity, uniform fin thickness, adiabatic cover plate, negligible radiation and convection heat transfer, uniform fin-base temperature, identical fin-base and channel-base temperature, and uniform coolant temperature and heat transfer coefficient at a given axial distance.<sup>13</sup>

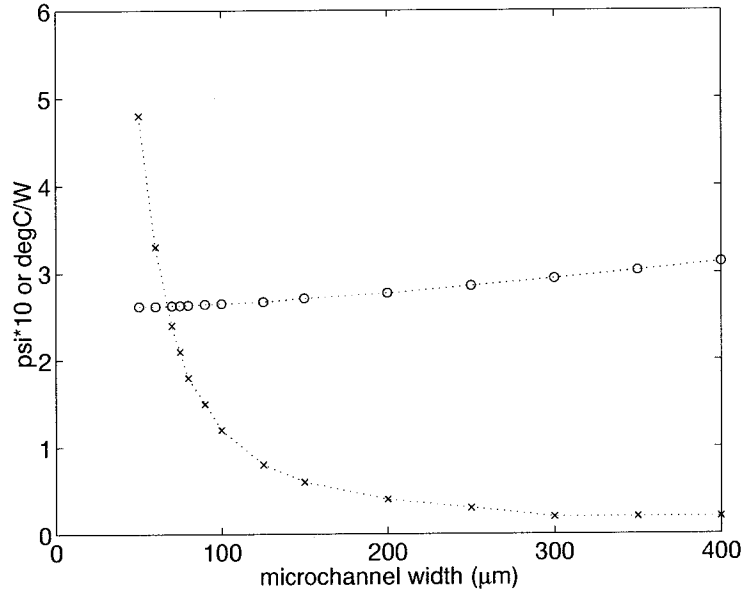


**Figure 5.** Results from the numerical model; (x) for the pressure drop and (o) for the total thermal resistance. For clarity, the numerical data has been connected with dotted lines. The microchannels are all 400 microns deep, and the microchannel spacing is equal to the width. The power density is 25 W/cm<sup>2</sup> and the flow rate is 20 cc/min.

#### 4.1. Hydraulic performance

The hydraulic performance of microchannel heat exchangers is characterized by the pressure drop,  $\Delta P$ . The total pressure drop is due to frictional losses, and losses from the working fluid passing through 90° bends and areas of sudden expansion and contraction. In the following calculations, only the frictional losses were considered since they were much greater than the others. The friction factor is a function of the microchannel aspect ratio and the Reynolds number; the fully developed laminar flow friction coefficients in rectangular ducts from Shah and London<sup>14</sup> were used.

#### 4.2. Thermal performance

The thermal performance of the microchannel heat exchangers is characterized by the total thermal resistance,  $R_{total}$ , where  $R_{total} = (T_{heater} - T_{in})/q$  and  $T_{heater}$  is the temperature of the heater,  $T_{in}$  is the bulk temperature of the fluid at the inlet, and  $q$  is the power applied. For these flows, the effects of viscous heating are negligible. The thermal resistance has three main components<sup>8</sup>: (1) conductive resistance through the substrate between the heated surface and the microchannel base plane,  $R_{cond}$ , (2) convective resistance from the microchannel surface to the working fluid,  $R_{conv}$ , and (3) temperature rise resistance from the bulk temperature rise of the working fluid from the device inlet,  $R_{heat}$ . The resistance  $R_{cond}$  is calculated by  $h_2/kA_h$  where  $h_2$  is the distance from the heated surface to the base of the microchannels,  $k$  is the thermal conductivity of the substrate, and  $A_h$  is the footprint of the microchannel heat exchanger. The resistance  $R_{conv}$  is calculated by  $1/h_c A_c$  where  $h_c$  is the convective heat transfer coefficient and  $A_c$  is the wetted area. The resistance  $R_{heat}$  is calculated by  $1/\dot{m}c_p$  where  $\dot{m}$  is the mass flow rate and  $c_p$  is the specific heat of the working fluid. The sum of these three resistances,  $R_{cond} + R_{conv} + R_{heat} = R_{total}$ . The convective resistance makes the largest contribution to  $R_{total}$ .

#### 4.3. Results

The model was validated by experimental data (see section 5) and then used as a design tool. Here we demonstrate use of the model to optimize a design from the Stanford University Microfluidics Laboratory. The design goal was to remove 25 W/cm<sup>2</sup> of heat without boiling the working fluid. Using a simple energy balance for the fluid,  $q = \dot{m}c_p(T_{out} - T_{in})$ , we find that the mass flow rate must be 20 cc/min if the fluid is water, the footprint of the

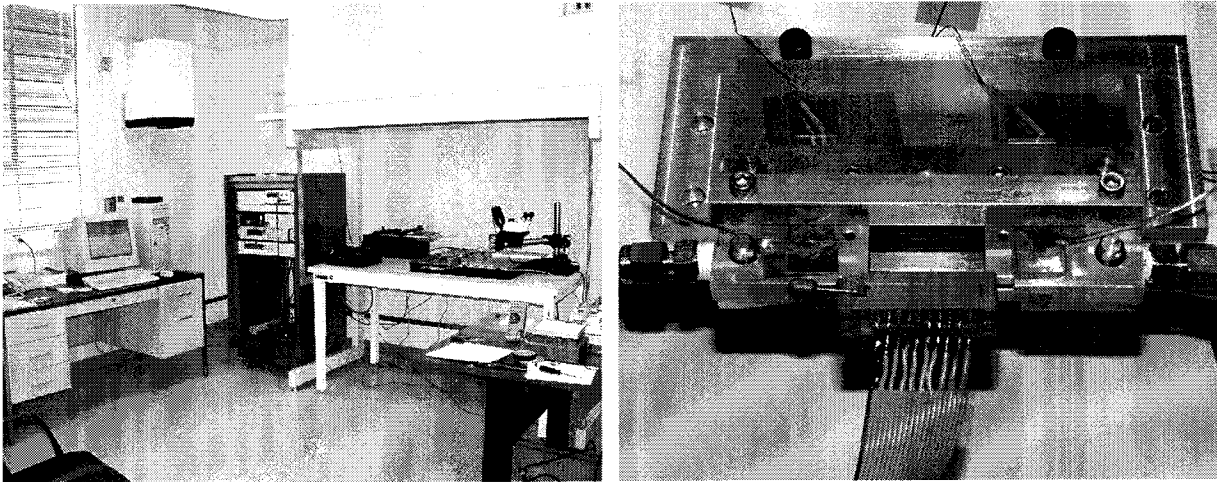


**Figure 6.** Photographs of the microchannel heat exchanger flow facility at JPL 18-101 (left) and a microchannel heat exchanger device clamped into the aluminum test fixture (right).

microchannel heat exchanger is  $3.5 \text{ cm}^2$ , and the temperature difference  $T_{out} - T_{in}$  is  $65 \text{ }^\circ\text{C}$ . To minimize the pressure drop, we etch the microchannels as deep as possible leaving enough substrate at the channel base to prevent device cracking or leaking. If the wafer thickness is 500 microns, it is possible to etch 400 micron channels. For simplicity, the microchannel spacing is set equal to the microchannel width. Results are presented in Figure 5; based on these results a width of 150 microns seems optimal since larger widths do not substantially reduce the pressure drop and the thermal resistance is increased.

## 5. EXPERIMENTS

The following sections describe the on-going experimental work with the MEMS-based liquid cooling system at the Jet Propulsion Laboratory (JPL).

### 5.1. Experimental facilities

The thermal and propulsion engineering section at JPL has developed a facility to examine components of microchannel heat exchanger systems (Fig. 6). The facility consists of a laminar flow bench, a test fixture, laboratory instrumentation, and a data acquisition system. The laminar flow bench provides a class 100 clean room environment for the microchannel device testing. An aluminum test fixture, procured by JPL through a contract with Stanford University Microfluidics Laboratory, uses two O-rings to create a seal at the inlet and the outlet to the microchannel device. The fixture was designed to accommodate microchannel devices with inlet and outlet holes spaced 4 cm apart. Internal passageways in the test fixture connect the microchannel device orifices to macroscopic,  $1/8''$  O.D. stainless steel tubing. De-ionized water at room temperature ( $22 \text{ }^\circ\text{C}$ ) is forced through the tubing and test fixture using a programmable syringe pump (Harvard Apparatus 70-2023 and 55-4208). The cooling fluid is exhausted to atmospheric pressure and the pressure drop across the test fixture is measured using a differential pressure transducer (Validyne DP15-50-N-1-5-4A) and carrier demodulator unit (Validyne CD15).

The test fixture was instrumented with six Type E thermocouples and two PT100 resistance temperature detectors (RTD). The thermocouples measure the inlet and outlet temperatures of the test fixture, and the lid and base temperatures of the fixture near both ends of the microchannel device. The RTDs are located on the upper surface of the aluminum test fixture and are used with a temperature controller (Lakeshore 340) to operate a “guard” heater element positioned under the test fixture. This guard heater may be used to elevate the temperature of the test fixture to match that of the microchannel heat exchanger device and reduce parasitic heating losses.

The surfboard pins on each microchannel heat exchanger device were attached to a Zero Insertion Force (ZIF) socket to establish electrical connections to the heaters and thermistors implanted in each device. A programmable

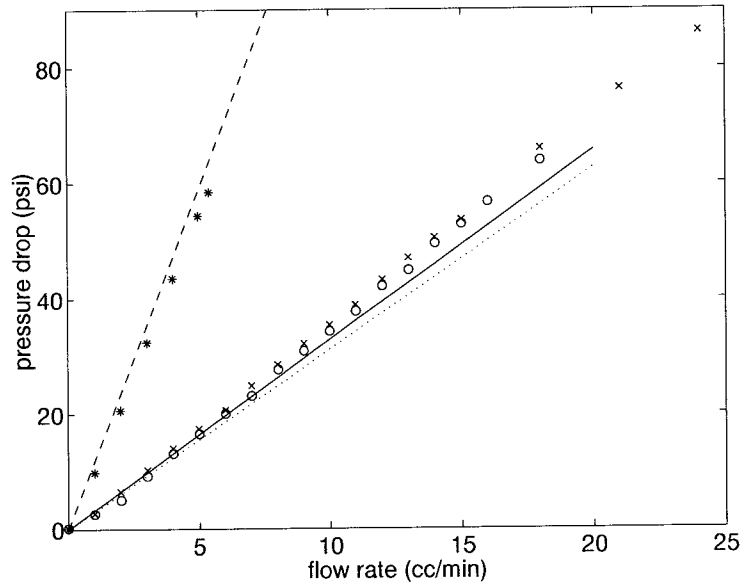


**Figure 7.** Experimental results showing pressure drop as a function of flow rate for three microchannel heat sink devices: (\*) for device 50-50-20, (x) for device 75-50-50, and (o) for device 100-50-30. The numerical results are indicated by lines: (- -) for device 50-50-20, (· · ·) for device 75-50-50, and (-) for device 100-50-30. The heaters were unpowered for these experiments.

power supply (Hewlett-Packard 6634A) was used to power the onboard heating elements and allowed for control of the input heating to the system. Although the thermistors were intended to provide in-situ measurements of the device temperature, they were found to be unreliable under test conditions. A third PT100 RTD was placed on the Pyrex surface of each microchannel heat exchanger device to measure the approximate chip temperature at the center of the device. The experiments were controlled and monitored using LabVIEW software in conjunction with a data logger (Fluke Hydra 2625A) and temperature controller.

## 5.2. Experimental procedures and results

The hydraulic performance of each microchannel heat exchanger device was assessed by measuring the pressure drop achieved for a given flow rate. For each test, a period of approximately five minutes was allowed for the flow within the device to achieve a steady state. Flow rates up to 25 cc/min were tested and the results are shown in Figure 7 along with the numerical predictions. It is clear from this data that the pressure drop across these devices is nearly linear with flow rate and characteristic of fully-developed laminar flow.

The thermal performance of the microchannel heat exchanger devices was determined by recording the temperature rise in both the chip and test fixture for a number of flow rates and heat fluxes. Steady-state conditions for each test were achieved by monitoring both the pressure drop across the device and the average chip temperature. Figure 8 shows the transient response of both quantities along with the temperature rise in the exit tubing for the 75-50-50 device at a flow rate of 9 cc/min and power input of 20 W. Oscillations in the pressure drop were always present and were caused by the unsteady motion of the syringe plungers. Most test runs were conducted for approximately one hour to ensure steady-state conditions.

Figure 9 shows the average temperature rise in the devices as the heat flux applied to the chips is varied. For these tests, guard heating was not used. The 50-50-20 device data show that high chip temperatures are achieved for modest flow rates, while the 100-50-30 and 75-50-50 device data show lower chip temperatures for greater flow rates. Figure 9 also shows data compiled from numerical predictions for each device. The agreement between the experimental data and the numerical predictions for both hydraulic and thermal testing indicates that the numerical model may be used as a design tool for future microchannel heat exchangers.

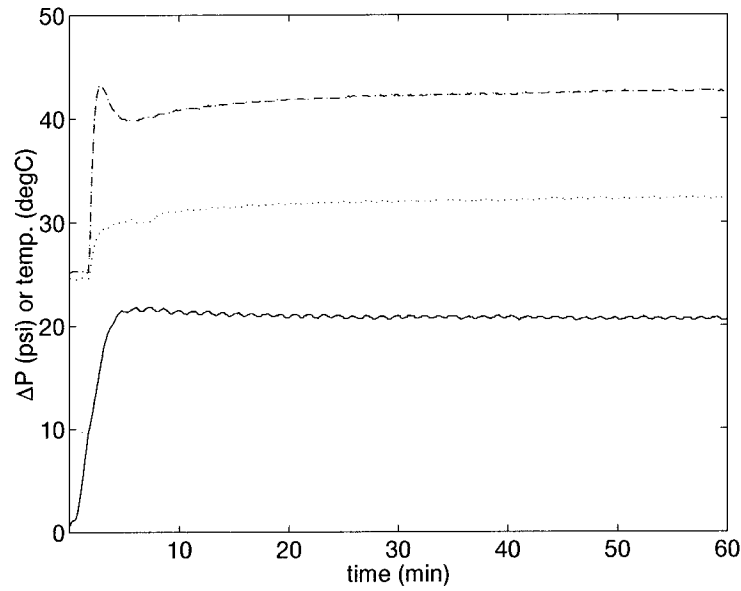


**Figure 8.** Typical experimental data for device 75-50-50: (—) for pressure drop, (---) for chip average temperature, and (···) for exit tubing temperature. The flow rate was 9 cc/min and 20W of power was applied.

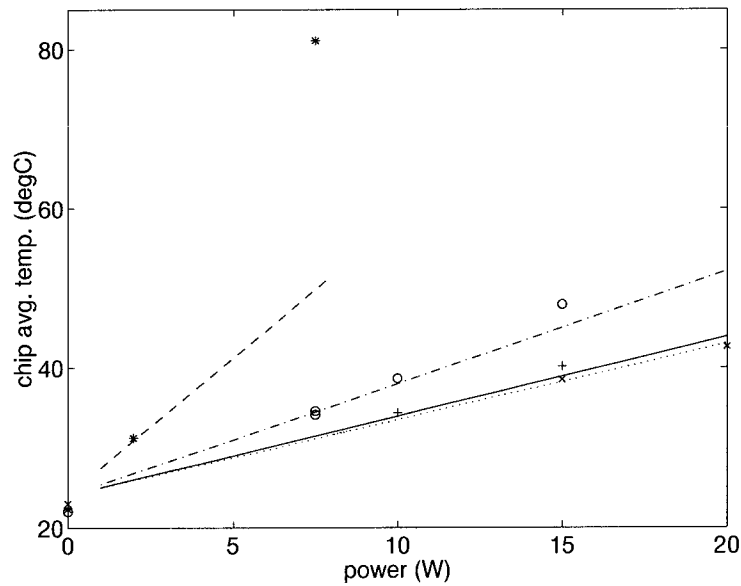


**Figure 9.** Experimental results showing chip average temperature as a function of power applied to the microchannel heat exchanger devices: (\*) for device 50-50-20 and 3 cc/min, (x) for device 75-50-50 and 9 cc/min, (o) for device 100-50-30 and 6 cc/min, and (+) for device 100-50-30 and 9 cc/min. The numerical results are indicated by lines: (---) for device 50-50-20 and 3 cc/min, (···) for device 75-50-50 and 9 cc/min, (- · -) for device 100-50-30 and 6 cc/min, and (-) for device 100-50-30 and 9 cc/min.

## 6. FUTURE WORK

At present, a batch of second generation microchannel heat exchanger devices is being fabricated at JPL. The configurations of these devices were based on the optimization studies discussed earlier and shown in Figure 5. These devices will be tested during the fall of 2001. In addition, several micropump technologies that are suitable for integration with the microchannels are being investigated. A few pumps of some of these technologies will be procured and tested in the JPL Microcooling lab during the latter part of 2001. In addition to the current microcooling "open-loop" testbed described in Section 5.1, a "closed-loop" test bed is being developed in the JPL Microcooling lab. The new test bed will be suitable for testing various microchannel heat exchanger devices and micropumps based on different technologies with various working fluids.

## 7. CONCLUSIONS

A MEMS-based pumped liquid cooling system suitable for microspacecraft thermal control applications is being developed at the Jet Propulsion Laboratory (JPL). The cooling system consists of a working fluid circulated through microchannels by a micropump. A numerical model was developed to predict the hydraulic and thermal performance of the microchannel heat exchanger devices used in this cooling system. First generation microchannel heat exchanger devices were fabricated and tested, and the experimental results are in excellent agreement with the numerical predictions. The preliminary results have shown that the single-phase liquid (water) cooling can remove heat fluxes of over 25 W/cm<sup>2</sup> from the electronic packages. The current focus of this ongoing investigation is using the numerical model as a design tool for optimization of the microchannel heat exchanger geometries and integrating a micropump which can provide the pressure head and flow rate required.

## ACKNOWLEDGMENTS

The research described in this paper was carried out at the Jet Propulsion Laboratory, California Institute of Technology, under a contract with the National Aeronautics and Space Administration. Funding was provided by NASA 632 Cross Enterprise Technology Development Program (Dr. Elizabeth Kolawa, Program Manager, Micro/Nano Sciencecraft Technology Program at JPL). The authors also wish to acknowledge technical support by Judy Podosek, Dr. Linda Miller, and Dr. Steven Vargo at JPL (Linda and Steven are now at Siwave Inc., Glendale, CA), and Professor Tom Kenny and Lian Zhang at Stanford University.

## REFERENCES

1. T. M. Harms, M. Kazmierczak, and F. M. Gerner, "Experimental investigation of heat transfer and pressure drop through deep microchannels in a (110) silicon substrate," *Proc. ASME Heat Transfer Division* **1**, pp. 347-357, 1997.
2. D. B. Tuckerman, *Heat-Transfer Microstructures for Integrated Circuits*. PhD thesis, Stanford University, Stanford, California, 1984.
3. M. Mahalingam, "Thermal managements in semiconductor device packaging," *Proc. IEEE* **73**, pp. 1396-1404, 1985.
4. T. Kishimoto and T. Ohsaki, "VLSI packaging technique using liquid-cooled channels," *IEEE Transactions on Components, Hybrids and Manufacturing Technology* **9**, pp. 173-181, 1986.
5. S. Sasaki and T. Kishimoto, "Optimal structure for microgrooved cooling fin for high-power LSI devices," *Electronics Letters* **22**, pp. 1332-1334, 1986.
6. R. A. Riddle, R. J. Contolini, and A. F. Bernhardt, "Design calculations for the microchannel heatsink," *Proc. National Electronic Packaging and Production Conference* **1**, pp. 161-171, 1991.
7. J. M. Cuta, W. D. Bennett, C. E. McDonald, and T. S. Ravigururajan, "Fabrication and testing of micro-channel heat exchangers," *Microlithography and Metrology in Micromachining SPIE* **2640**, pp. 152-160, 1995.
8. D. B. Tuckerman and R. F. W. Pease, "High-performance heat sinking for VLSI," *IEEE Electron Device Letters* **EDL-2(5)**, pp. 126-129, 1981.
9. J. S. Goodling, "Microchannel heat exchangers—a review," *SPIE High Heat Flux Engineering II* **1997**, pp. 66-82, 1993.

10. G. Birur and T. O'Donnell, "Advanced thermal control technologies for space science missions at Jet Propulsion Laboratory," in *Proc. Space Technology Application International Forum 2001, Albuquerque, NM*, M. El-Genk, ed., American Institute of Physics, 2001.
11. L. Zhang, S. Banerjee, J.-M. Koo, D. Laser, M. Asheghi, K. Goodson, J. Santiago, and T. Kenny, "A micro heat exchanger with integrated heaters and thermistors," *Proc. Solid-State Sensor and Actuator Workshop*, 2000.
12. R. J. Phillips, "Forced-convection liquid-cooled microchannel heat sinks," Master's thesis, Massachusetts Institute of Technology, Cambridge, Massachusetts, 1987.
13. R. J. Phillips, "Microchannel heat sinks," in *Advances in thermal modeling of electronic components and systems*, A. Bar-Cohen, ed., vol. 2, pp. 109–184, Hemisphere Publishing Corp., New York, 1990.
14. R. K. Shah and A. L. London, "Laminar flow forced convection in ducts," in *Advances in heat transfer*, J. P. Hartnett, ed., Academic, New York, 1978.